

## Numerical study of super-critical carbon dioxide flow in stepped-staggered labyrinth seals

Yuming Zhu<sup>a,b</sup>, Yuyan Jiang<sup>a,\*</sup>, Shiqiang Liang<sup>a</sup>, Yongxian Guo<sup>a</sup>, Chaohong Guo<sup>a</sup>, Peng Yue<sup>a</sup>

<sup>a</sup> Institute of Engineering Thermophysics, Chinese Academy of Sciences

<sup>b</sup> University of Chinese Academy of Sciences

### ABSTRACT

In this paper, a new kind of axial labyrinth seals, called stepped-staggered labyrinth seals, has been described to reduce process gas escaping from the shaft end of SCO<sub>2</sub> compressor, and numerical study of super-critical carbon dioxide flow(SCO<sub>2</sub>) has been applied to evaluate its performance compared to see-through labyrinth. The computational fluid dynamic(CFD) calculations were carried out using the NUMECA commercial code. To minimize the computational cost and keep the desired level of accuracy in the characterization, the NIST REFPROP database was used for the computation of SCO<sub>2</sub> in the numerical investigation. It can be observed that throttling effect exists in both seal clearance and shoulder clearance, and strong vortex flow occurs at staggered cavity. So, the Stepped-staggered labyrinth seals have better seal performance than see-through labyrinth and avoid the assembly problem of axial interlocking labyrinth. Finally, Various designs with different structure parameters and conditions have been calculated to explore the primary design method of stepped-staggered labyrinth seals. For the test platform is under construction, experimental results of stepped-staggered labyrinth seals are not available. To prove the potential of the methodology, see-through cases on this numerical model have been operated and indicate a very good agreement with the existing see-through labyrinth seals experiment results.

### INTRODUCTION

Numerous studies have shown that these SCO<sub>2</sub> power cycles have the potential to attain significantly higher cycle efficiency than either a conventional steam Rankine cycle or even the ultra-super-critical (USC) steam Rankine cycle over a wide temperature range of heat sources with compact components resulting in a smaller system footprint, lower capital and operating costs [1,2]. A Typical SCO<sub>2</sub> power cycle is showed as fig.1, which operates a cycle in super-critical region [3].

The critical pressure of CO<sub>2</sub> is 7.38MPa and the maximum pressure of cycle may up to 20MPa, so the SCO<sub>2</sub> compressor's operation pressure is much higher than that of traditional air compressor. Besides, the kinematic viscosity of SCO<sub>2</sub> is much smaller than air, as is shown in table.1, which will lead to a much thinner boundary layer and may increase the leakage of seal. Labyrinth seal is a kind of typical mechanical seal, widely used in turbo-machinery. And there are many different type of labyrinth seal, such as see-through labyrinth seal, stepped labyrinth seal, staggered labyrinth seal and so on. *Haomin Yuan(2015)* studied the see-through labyrinth seal used in SCO<sub>2</sub> flow in fig.2 both numerically and experimentally. In the Sandia National Laboratory (SNL) SCO<sub>2</sub> Brayton cycle experiment loop [5] a stepped labyrinth seal is adopted for its compressor as shown in Fig.3. For the cases operating in high pressure condition, see-through or stepped labyrinth seal may hard to meet the requirement of leakage.

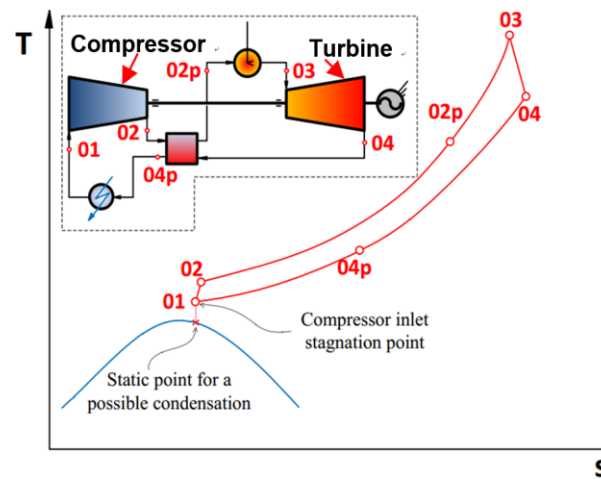


Fig.1 Typical SCO<sub>2</sub> power cycle (T-S)

**Table 1**

The properties of air and  $\text{SCO}_2$

	Temperature	Pressure	Density	Viscosity	Kin. Viscosity
	(K)	(MPa)	( $\text{kg/m}^3$ )	( $\mu\text{Pa}\cdot\text{s}$ )	( $\text{cm}^2/\text{s}$ )
<b>Air</b>	320	10	108.26	21.492	0.0019852
<b><math>\text{SCO}_2</math></b>	320	10	448.28	32.388	0.00072251

Axial staggered labyrinth is one of the most powerful labyrinth seal, which is always used in large-scale machinery with split cases in fig.4. As the  $\text{SCO}_2$  turbine machines have the characteristics of smaller volume and high running speed, turbine rotor system is sensitive to the case assembly error. It is difficult to ensure installation accuracy for the small-scale split case, so it is in an urgent need for us to develop new kind of axial labyrinth seals to resolve the assembly problem of axial staggered labyrinth and to meet the acquirement of high pressure seal in high speed shaft end. In this paper, a stepped-staggered labyrinth

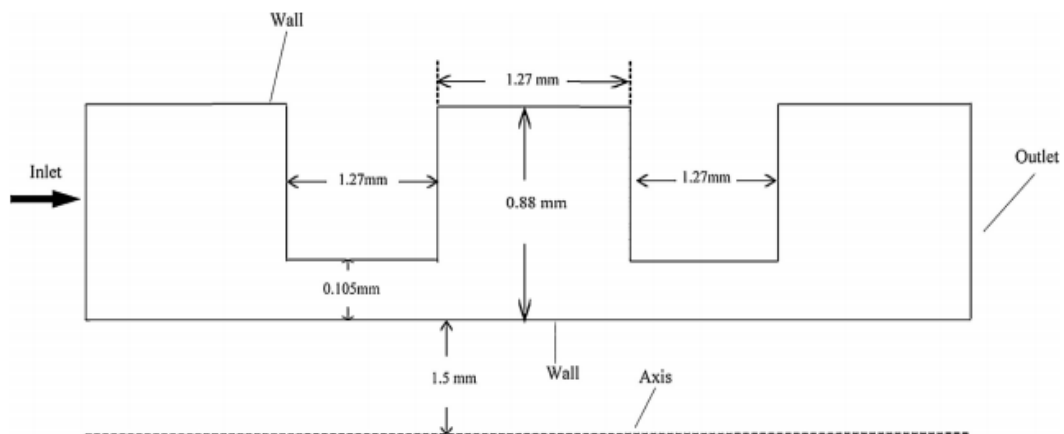


**Fig.2** The see-through labyrinth seal in *Haomin Yuan's* paper

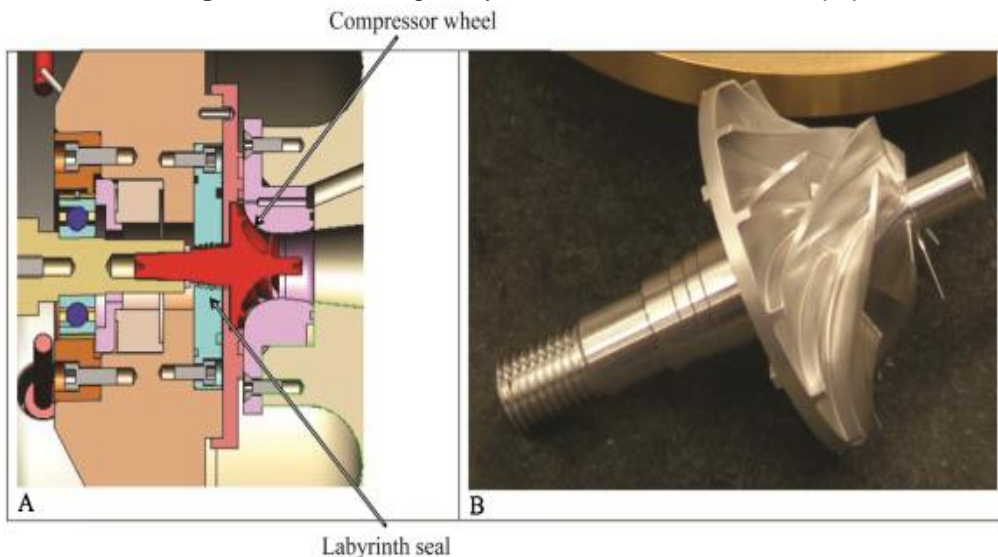


**Fig.3** Stepped labyrinth seal used in SNL  $\text{SCO}_2$  Brayton cycle experiment loop

seal has been developed, as it is shown in fig.5, this new seal uses stepped structure to avoid the assembly problem and form a staggered chamber in each step to reduce the shaft end leakage, which combines the advantages of stepped and staggered labyrinth seal.

Unlike the numerical research of traditional air labyrinth seal, the unique fluid behavior of  $\text{SCO}_2$  near its critical and pseudo-critical points challenges its numerical modeling [4]. In this paper, an accurate property database including the property of super-critical and two-phase region has been developed using NIST REFPROP database. And the computational fluid dynamic(CFD) calculations were carried out using the NUMECA commercial code to simulate the phase-change process which is the key for the numerical simulation results.

For the test platform is under construction, experimental results of stepped-staggered labyrinth seals are not available. In this paper, we use the experimental results of  $\text{SCO}_2$  flow in see-through labyrinth seals from Haomin Yuan's research, as is shown in fig.2[4]. The same see-through structure cases in fig.8 have been operated, and the numerical results have been compared with the above-mentioned experimental results to prove the potential of the methodology.

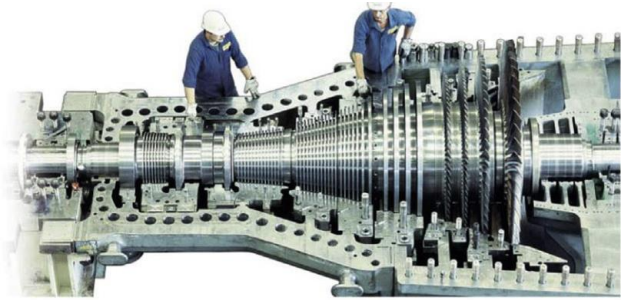


**Fig.4** Large-scale machinery with split cases

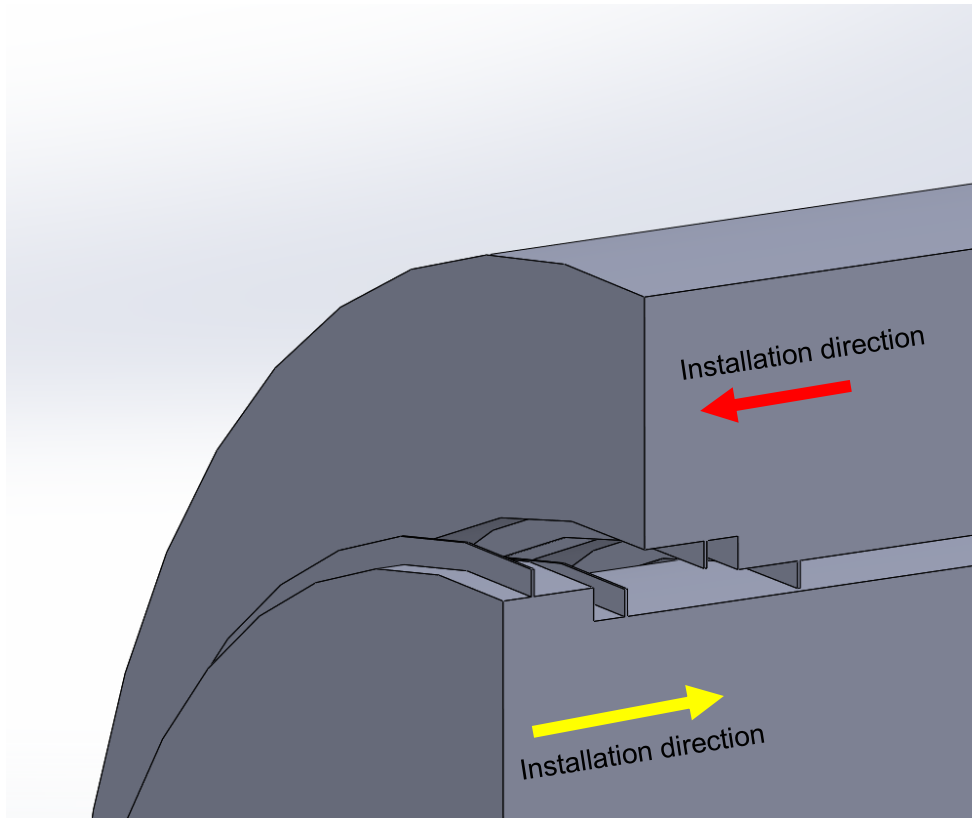


**Fig.5** Stepped-staggered labyrinth seal

## Numerical methodology and availability

This chapter describes and discusses the numerical procedure used in this investigation. The first section introduces Navier-Stokes equations and solver algorithm. The second part moves on to describe in detail about the property module of  $\text{SCO}_2$  and phase-change model. Then different turbulence models will be compared. After that the mesh independent problem will be studied and discussed. And this chapter ends with a comparison between the numerical results and experimental results to prove the availability of the numerical method used in this paper. In this chapter, the inlet condition of see-through structure cases used to verify the availability of the numerical model is set as (10MPa, 320K).

### 2.1 Navier-Stokes equations and solver algorithm

The fluid is simulated using the Reynolds Averaged Navier–Stokes (RANS) equations, applied to a rotating system. For the single rotating reference frame simulation, the governing equations based on relative velocity are given by:

#### Mass conservation

$$\nabla \cdot (\rho \mathbf{V}_r) = 0$$

#### Conservation of momentum

$$\nabla \cdot (\rho \mathbf{V}_r \mathbf{V}_r) + \rho (2\boldsymbol{\omega} \times \mathbf{V}_r + \boldsymbol{\omega} \times \boldsymbol{\omega} \times \mathbf{r}) = -\nabla P + \nabla \cdot \boldsymbol{\tau}$$

#### Conservation of energy

$$\nabla \cdot (\rho H \mathbf{V}_r) + \nabla \cdot \left( \rho \frac{1}{2} \mathbf{V}_r^2 \mathbf{V}_r \right) + \nabla \cdot \left( \rho \frac{1}{2} \mathbf{U}_r^2 \mathbf{V}_r \right) = k \nabla T + \nabla \cdot (\boldsymbol{\tau} \cdot \mathbf{V}_r)$$

where  $\mathbf{V}_r$  is defined as:

$$\mathbf{V}_r = \mathbf{V} - \mathbf{U}_r$$

$$\mathbf{U}_r = \boldsymbol{\omega} \times \mathbf{r}$$

### 2.2 Model of physical properties

As is reported in [7,8], they used NIST Refprop to formulate a  $\text{CO}_2$  equation into a two-dimensional table for simulations. The advantage of this method is that the fineness of the table can be controlled by adjusting the number of sampling points in the table and the temperature and pressure ranges covered by the table. Compared with the method of directly invoking the state equation, the method keeps the calculation precision and save the calculation time-consuming. In this paper, we use a software in

**Table 2**  
Two physical tables with different resolutions

	P Range	T Range	Points
	MPa	K	n
<b>Table 1</b>	0.005-800	216-2000	101
<b>Table 2</b>	4-20	270-500	101

NUMECA called TabGen to generate CO<sub>2</sub> property tables. To study the impact of the resolution of CO<sub>2</sub> property tables on the CFD results accuracy, we make two physical tables with different resolutions, as is shown in table.2, and operate see-through structure cases with the outlet pressure of 7MPa.

The numerical results using property tables with different resolutions are showed in table.3. We can find that the difference of leakage is negligible and both are close to the experimental result, so the resolution of property tables may have no effect on calculation precision, which is different from the impact on near-critical compressor. To minimize the computational cost and keep the versatility of property tables, the property tables (range from 0.0005MPa to 800MPa and from 216K to 2000K) are used for the computation of SCO<sub>2</sub> in the numerical investigation

**Table 3**

The numerical results using property tables with different resolutions

	<b>Table 1</b>	<b>Table 2</b>	<b>Experiment Result</b>
<b>Leakage ( kg/s )</b>	0.03369	0.033359	0.33

Besides, in NUMECA, the simulation of the physical properties using condensable fluid model to solve the phase-change condition. This model enables the simulation of complex thermodynamic properties by interpolating variables from specialized tables. Condensable fluid models are suitable for single-phase fluids where the real gas properties are too complex to be modeled as ideal gas models or polynomial fit. This modeling method is more accurate for the calculation of the liquid or gaseous zone near the two-phase zone. When the calculated fluid state is in the two-phase region, the fluid state is considered as a two-phase mixture that is uniformly balanced in gas and liquid. When an equilibrium mixture of steam and liquid droplets, such as wet steam, is considered as a single fluid, its saturated state thermodynamic variables must be iteratively calculated.

### 2.3 Turbulence model

In NUMECA, the solver is designed for RANS turbulence model and provides various turbulence model to choose from. To find out the most suitable turbulence model for the case, we select four different types of turbulence models: Spalart-Allmara, SARC, k-epsilon (Extended Wall Function), k-omega (M-SST, Extended Wall Function), and operate see-through structure cases with the outlet pressure of 7MPa. The numerical results using different turbulence model are showed in table.4. We can find that the numerical result with Spalart-Allmara turbulence model is much closer to the experimental result. Therefore, the Spalart-Allmara turbulence model is used to study the performance of stepped-staggered labyrinth seals.

**Table 4**

The numerical results using different turbulence model

	<b>Spalart-Allmara</b>	<b>SARC</b>	<b>k-epsilon</b>	<b>k-omega</b>	<b>Experimental Result</b>
<b>Leakage(kg/s)</b>	0.033359	0.03238	0.03239	0.03127	0.033

## 2.4 Mesh independent

To verify the mesh independent and obtain the average number of computational mesh required, three different number of grids have been meshed and each grid number is Mesh1 = 14289, Mesh2 = 25833 and Mesh3 = 63348. In order to compare with the experimental data, we operate see-through structure cases with the outlet pressure of 7MPa. The numerical results using physical tables with different resolutions are showed in table.5. From the table, we can find that it will lead to significant error when the mesh is too coarse, so the mesh with mesh number above 30000 is recommended.

**Table 4**

The numerical results with different number of grids

	Mesh1	Mesh2	Mesh3	Experimental Result
<b>Leakage(kg/s)</b>	0.03145	0.033359	0.03282	0.033

## 2.5 Method availability

To fully evaluate the availability of the above-stated numerical method, more outlet pressure condition has been operated. And the numerical results operated by NUMECA has been compared with the see-through labyrinth seal experimental data and the numerical results operated by OpenFOAM reported in *haominyuan*[4] shown in fig.6 (in the picture, the red point represent the numerical results operated by NUMECA, the black point represent the numerical results operated by NUMECA and the blue point represent the experimental data). The results operated by numerical method used in this paper shows high degree of coherence with the see-through labyrinth seal experimental data, which proves that this method is feasible and reliable.

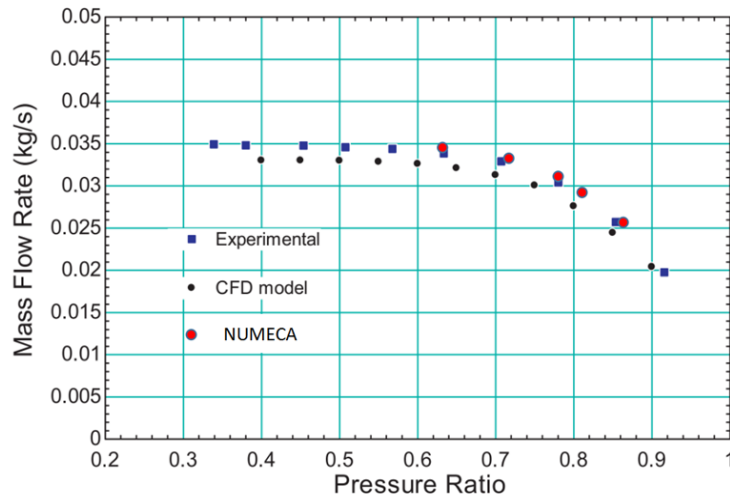


**Fig 6** The experimental data and the numerical results operated by NUMECA and OpenFOAM

## RESULTS AND DISCUSSION

In this chapter, the research structures are described, and numerical results are presented and discussed. First, the detail structure of stepped-staggered labyrinth seal and some structure characteristic parameters are introduced. Then, we compare performance between see-through and the new stepped-staggered labyrinth, and try to explain the difference from details of the flow, including pressure distribution and stream line plot. After that, various designs with different structure parameters and conditions have been calculated to explore the primary design method of stepped-staggered labyrinth seals.

### 3.1 Structure of stepped-staggered labyrinth seal

As is shown in fig.7, a two-step stepped-staggered labyrinth seal is used to investigate the seal performance and design method of this new seal, and we chose 3 characteristic variables and 4 non-dimensional numbers to describe its detail structure (see table 1). From fig.10, we can find that the installation direction of case wall and shaft wall is opposite, leaving an installation clearance “e” which is one of the main features of the new seal. In this research, we focus on three non-dimensional numbers ( $a/b$ ,  $c/b$ ,  $d/b$ ) and make a primary qualitative research. And the quantitative analysis of effects of 7 variables (including 3 characteristic variables and 4 non-dimensional numbers) will be studied in our future work.

**Table 5** The 7 structure variables of stepped-staggered labyrinth seal

	definition	units
$a/b$	Radial clearance between shaft and case/ Cavity height	/
$c/b$	Cavity length/ Cavity height	/
$d/b$	Tooth width/ Cavity height	/
$e/b$	Axial clearance between shaft and case/ Cavity height	/
$n$	Step number	/
$r$	Shaft radius	m
$b$	Cavity height	m

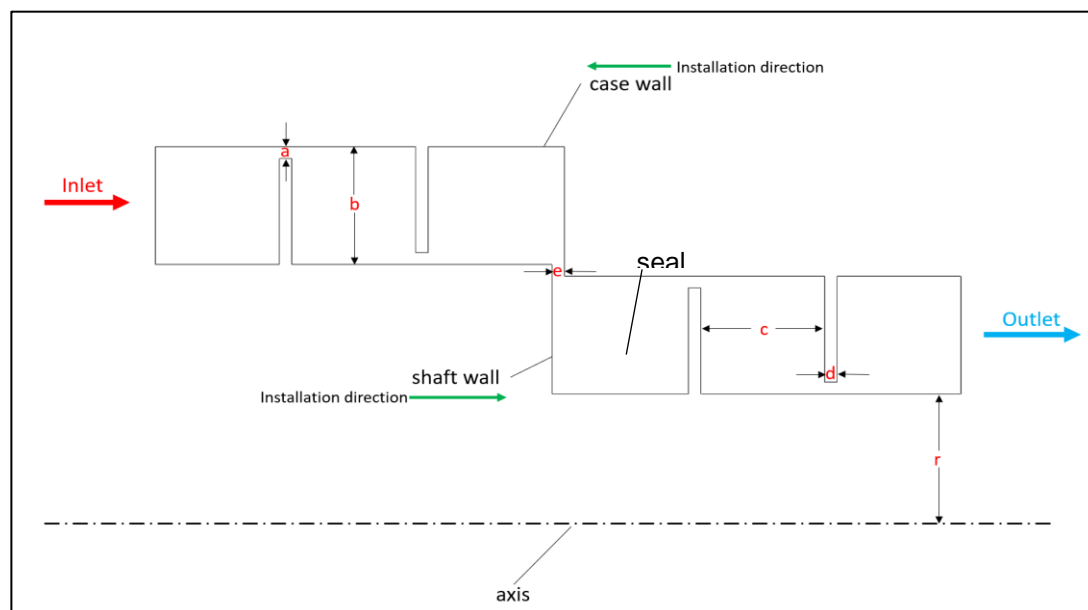


**Fig 7** The structure of stepped-staggered labyrinth seal

### 3.2 Comparison of sealing performance

To compare the sealing performance of see-through and the new stepped-staggered labyrinth seal, we operate a five-tooth see-through labyrinth in fig.8 with six seal cavities which is the same as the two-step stepped-staggered labyrinth seal in fig.7. Considering the seal size used in actual turbine machine, we set

**Table 6** The value of stepped-staggered labyrinth seal characteristic dimensions

a/b	c/b	d/b	e/b	n	r	b
0.1	1	0.1	1	2	30mm	1mm

the shaft radius of all seals to 30mm and the others dimensions are shown in table.6.

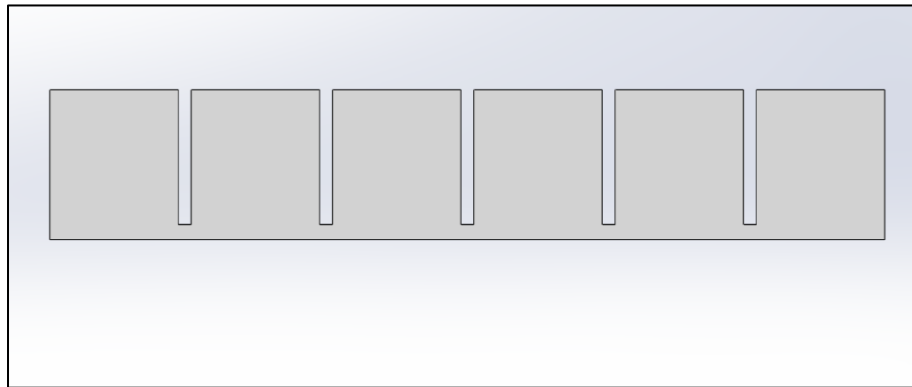


**Fig 8** The structure of five-tooth see-through labyrinth

In this study, the inlet operating condition is fixed at (10 MPa, 320K) and the outlet pressure ranges from 4MPa to 7MPa. The numerical results are presented in fig.9, and it would be easy to conclude that the new stepped-staggered labyrinth seal has better sealing performance than see-through with the same seal clearance and sealing length. The relative Mach number plots obtained by the CFD in fig.10 also prove the validity of this point. From fig.10, we can find that the relative Mach number distribution of the new labyrinth seal is much more dispersive, which means a much stronger viscous dissipation occurring in seal cavity, so the Mach number is smaller and the seal effect is better.

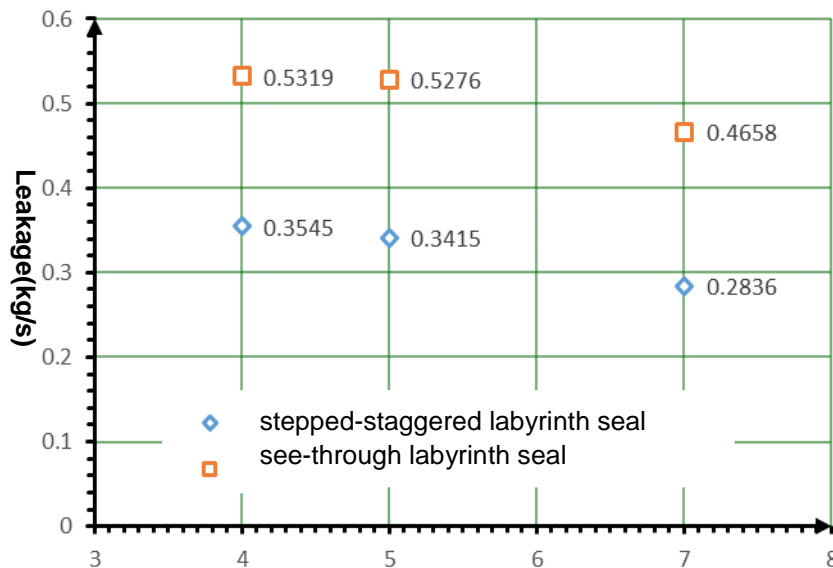


**Fig 9** The numerical results of stepped-staggered and see-through labyrinth seal



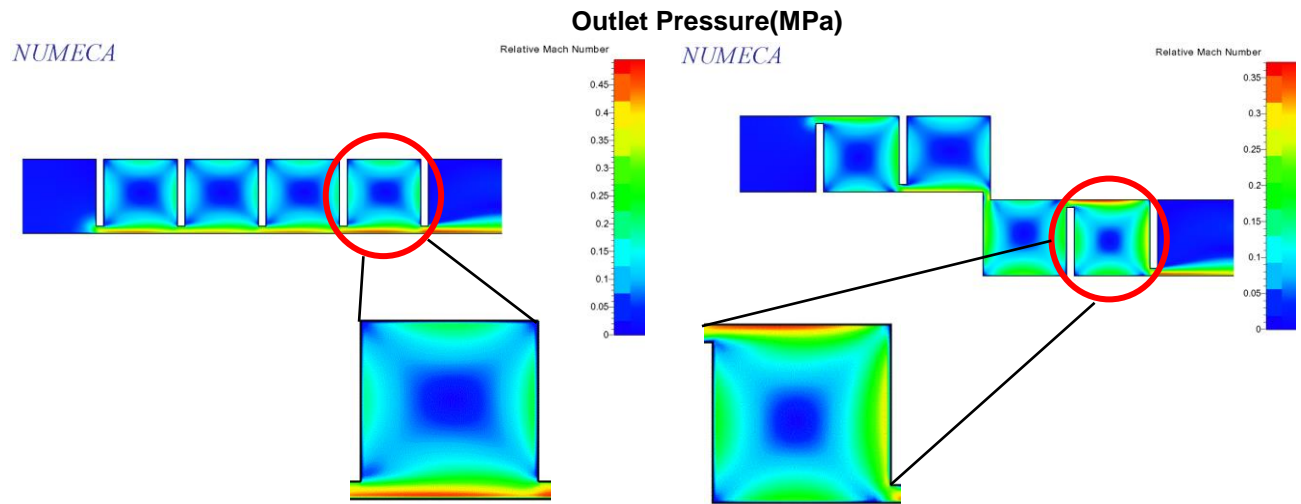


**Fig 10** The relative Mach number distribution of stepped-staggered and see-through labyrinth seal

### 3.3 Clearance ratio

The data in Fig.11 shows that, the leakage rate increases with increase in radial clearance. This is a fairly obvious result as an increase in clearance area allows more fluid to be forced underneath the tooth. And it should be pointed that it is approximate to a linear development between leakage and clearance, when the shaft radius is large enough.

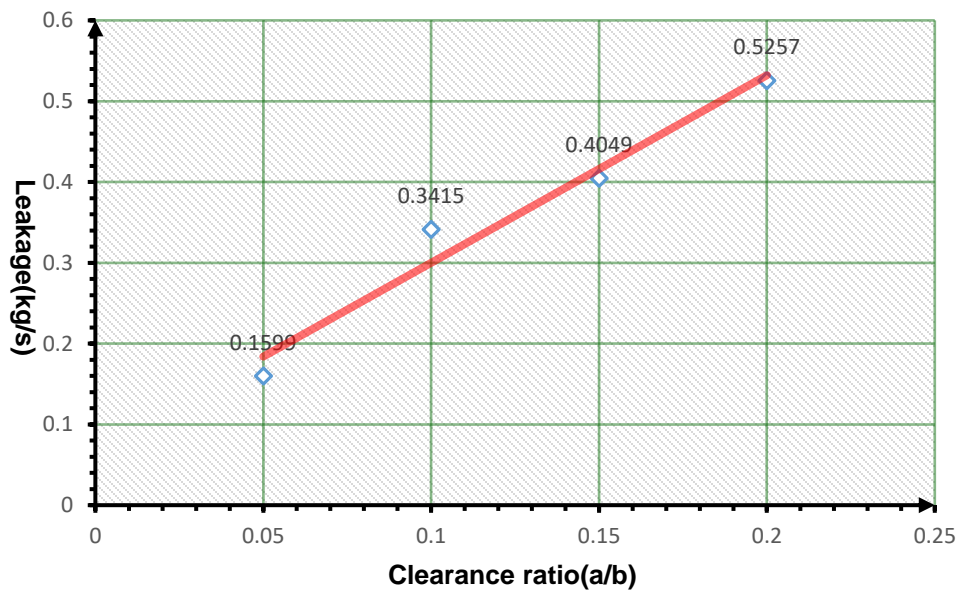


**Fig 11** The numerical results of stepped-staggered and see-through labyrinth seal

### 3.4 Length/height ratio

The numerical results of labyrinth with different length/height ratio are compared in fig.12, and we can find that the seal performance is worst when length/height ratio is equal to 1, which means a square sealing cavity. Furthermore, it is remarkable that the leakage of the seal (length/height ratio=0.5) is very close to that of the seal (length/height ratio=2). And if we show the data in a log coordinate, as is presented in fig.13, the sealing performance exhibits pretty good symmetry of geometric topology, which is a unique rule and can be a powerful tool to design high-performance mechanical seal.

Though two seals above with similar geometric topology show the same sealing performance, they have the different flow mechanisms as are shown in fig.14. From the streamline patterns, it is obvious that the seal (length/height ratio=0.5) has stronger vortex effect and even emerge additional vortex near the seal clearance and the seal (length/height ratio=2) has a double sealing length to earn a “double” sealing effect.

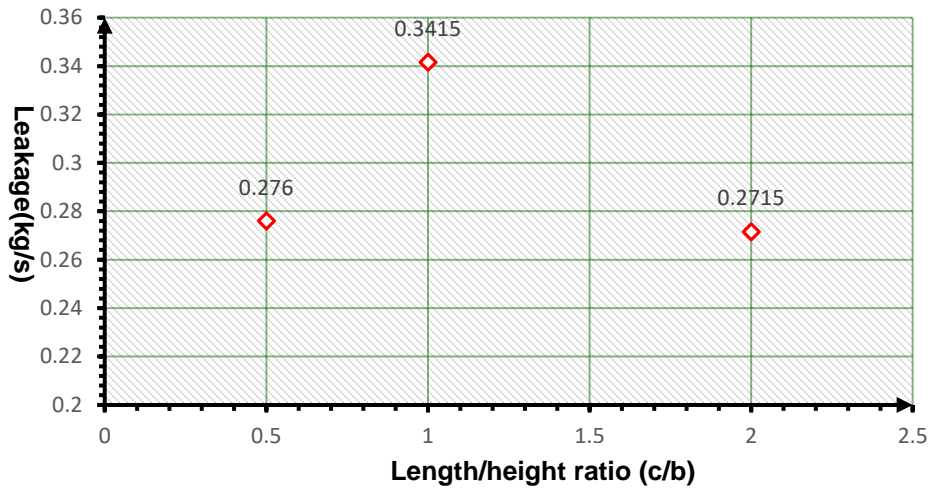


Fig 12 The numerical results of labyrinth with different length/height ratio

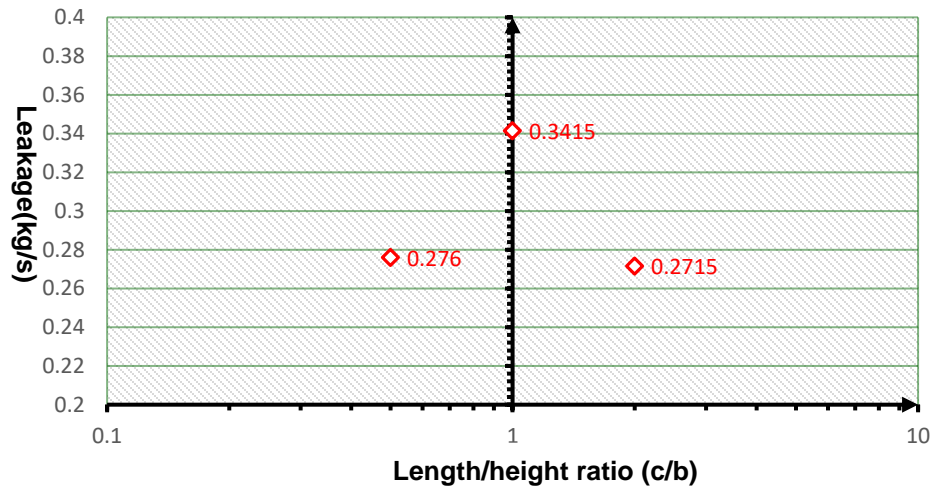
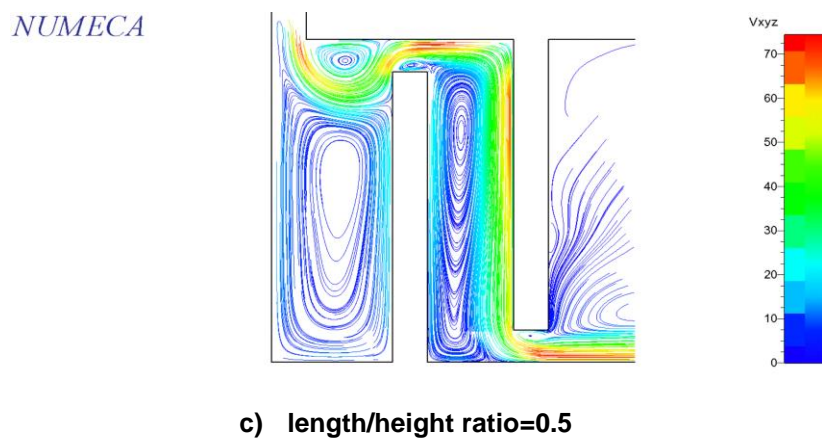
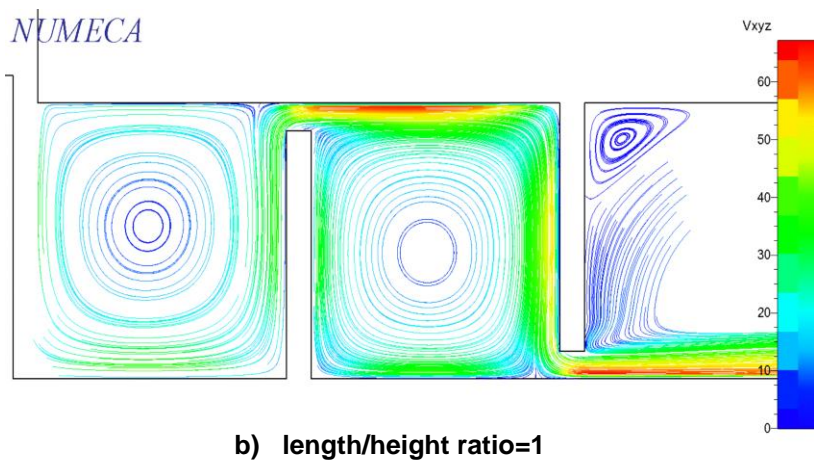
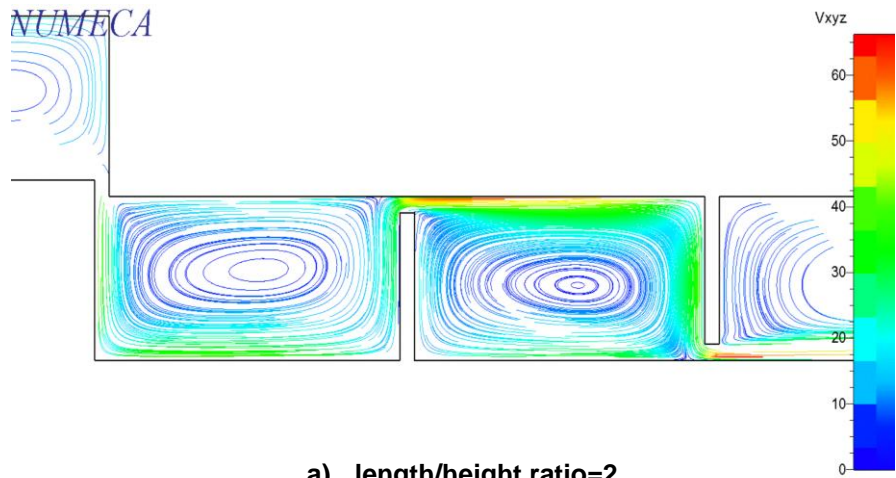


Fig 13 The numerical results of labyrinth with different length/height ratio (in a log coordinate)



**Fig 14** The streamline patterns of cases with different length/height ratio

### 3.5 Tooth width/height ratio

The numerical results of labyrinth with different tooth width/height ratio are compared in fig 15, and we can find the rule of seal leakage with change of tooth width/height ratio is similar with that of length/height ratio, which means that it may exist a best width/height ratio which will lead to the least leakage. It is clear that the seal (width/height ratio=5) has a double sealing length where the speed of flow is extremely high, and it will lead to an increase of the friction loss. When the width/height ratio is very small, the throttling effect must be enhanced, and the sealing performance is boosted.

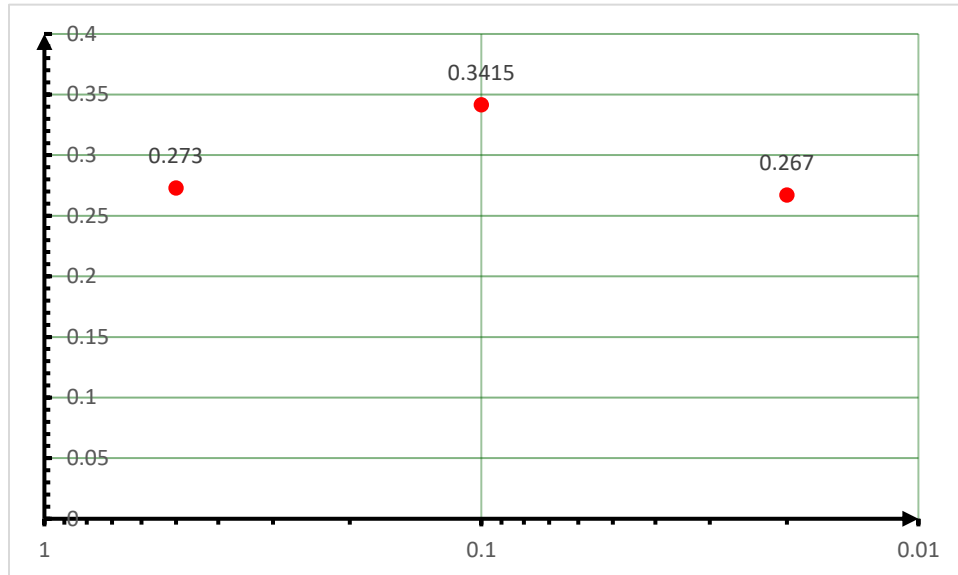


**Fig 15** The numerical results of labyrinth with different tooth width/height ratio (in a log coordinate)

### 3.6 Conclusions

- A. The new stepped-staggered labyrinth seal has better sealing performance than see-through with the same seal clearance and sealing length.
- B. The leakage rate increases with increase in radial clearance.
- C. The seal performance is worst when length/height ratio is equal to 1, and the sealing performance shows a good symmetry of geometric topology with length/height ratio.
- D. It may exist a best width/height ratio which will lead to the least leakage.

## REFERENCE

- [1] Fundamentals and Applications of Super-critical Carbon Dioxide (SCO<sub>2</sub>) Based Power Cycles.
- [2] Supercritical CO<sub>2</sub> Power Cycle Developments and Commercialization: Why ScCO<sub>2</sub> can Displace Steam.
- [3] Monje, B., Sánchez, D., Savill, M., Pilidis, P., & Sánchez, T. (2014). A Design Strategy for Supercritical CO<sub>2</sub> Compressors. ASME Turbo Expo 2014: Turbine Technical Conference and Exposition (pp.V03BT36A003-V03BT36A003). American Society of Mechanical Engineers.
- [4] Yuan, H., Pidaparti, S., Wolf, M., Edlebeck, J., & Anderson, M. (2015). Numerical modeling of supercritical carbon dioxide flow in see-through labyrinth seals. Nuclear Engineering & Design, 293, 436-446.
- [5] Wright, S. A., Radel, R. F., Vernon, M. E., Pickard, P. S., & Rochau, G. E. (2010). Operation and analysis of a supercritical co<sub>2</sub> brayton cycle. Sand.
- [6] Fairuz, Z. M., & Jahn, I. (2016). The influence of real gas effects on the performance of supercritical co<sub>2</sub>, dry gas seals. Tribology International, 102, 333-347.
- [7] Rinaldi E, Pecnik R, Colonna P. Exact Jacobians for implicit Navier–Stokes simulations of equilibrium real gas flows[J]. Journal of Computational Physics, 2014,270: 459-477.
- [8] E. Rinaldi R P, P. Colonna. Accurate and efficient look-up table approach for dense gas flow simulations[C]. ECCOMAS 2012 - European Congress on Computational Methods in Applied Sciences and Engineering, 2012

## ACKNOWLEDGEMENTS

This study was supported by the Institute of Engineering Thermophysics, Chinese Academy of Sciences SCO<sub>2</sub> Program (No. Y754026Z11). The authors would like to thank for their support for this research.